MDPI

Article

Selection for protein stability enriches for epistatic interactions

Anna Posfai [1], Juannan Zhou [1], Joshua B. Plotkin [2], Justin B. Kinney [1] and David M. McCandlish [1,*]

[1] Simons Center for Quantitative Biology, Cold Spring Harbor Laboratory, Cold Spring Harbor, NY, 11724
[2] Department of Biology, University of Pennsylvania, Philadelphia, PA, 19104
* Correspondence: mccandlish@cshl.edu; Tel.: 1+516-367-5286

Academic Editor: name
Version June 3, 2018 submitted to Genes

Abstract: A now classical argument for the marginal thermodynamic stability of proteins explains the distribution of observed protein stabilities as a consequence of an entropic pull in protein sequence space. In particular, most sequences that are sufficiently stable to fold will have stabilities near the folding threshold. Here we extend this argument to consider its predictions for epistatic interactions for the effects of mutations on the free energy of folding. Although there is abundant evidence to indicate that the effects of mutations on the free energy of folding are nearly additive and conserved over evolutionary time, we show that these observations are compatible with the hypothesis that a non-additive contribution to the folding free energy is essential for observed proteins to maintain their native structure. In particular through both simulations and analytical results, we show that even very small departures from additivity are sufficient to drive this effect.

Keywords: thermodynamic stability, epistasis, molecular evolution, purifying selection

1. Introduction

The relationship between protein sequence, stability, and function has been a subject of intense investigation for decades. A combination of biophysical and evolutionary models and, more recently, high-throughput mutagenesis experiments have dramatically advanced our understanding of this complex relationship [1–5]. A consensus view has emerged on some aspects of protein functions and evolution— e.g., what accounts for the distribution of thermodynamic stabilities observed in nature. And yet other questions—e.g., whether genetic interactions play a dominant or minor role in protein sequence evolution—remain actively debated, with apparently contradictory empirical and theoretical evidence [1–5].

A nuanced appreciation of the high-dimensional nature of protein sequence space has been essential for resolving questions about protein structure, function, and evolution. The observation that naturally occurring proteins are only marginally, as opposed to maximally, stable was first interpreted as an adaptive feature to permit increased protein flexibility and functionality [6]. But, with some exceptions [7], this view has been largely replaced with a more parsimonious explanation based on the high dimensionality of sequence space: marginal stabilities are observed because, simply, far more sequences are marginally stable than maximally stable [8]. Essential to the development of this explanation was the concept of sequence entropy [9,10] – the idea that the sheer number of protein sequences that map to a given phenotype exerts a strong entropic pull on the distribution of observed phenotypes in viable proteins[11–13]. The field today has mostly settled on a synthetic understanding of how simple biophysical models of energy and folding, along with the structure of sequence space, conspire to explain the distribution of protein stabilities observed in nature [1–5].

By contrast to observed stabilities, the role of epistasis in protein evolution and function remains a topic of active debate with unresolved ambiguities. The same bio-physical models that can parsimoniously explain observed distributions of stabilities have been reported to show only a weak context-dependence of mutational effects on stability [14], or, alternatively, reported to show very strong context dependence of mutational effects [13,15,16]. Likewise, experimental studies on the fitness effects of mutations in divergent sequence backgrounds have reportedly very weak epistasis [14], whereas comparative analysis of divergent proteins has implicated an overriding role for epistasis in shaping sequence evolution[17]. How are we to resolve this significant discrepancy about the role of epistasis for protein stability and sequence evolution?

In this paper we address this discrepancy by analyzing simple models for the relationship between amino acid sequence and the ΔG of folding. Under selection to maintain a minimum degree of stability, these models predict distributions of folding energies that are roughly consistent with those observed in nature. Moreover, the models predict very weak interactions between pairs of mutations. These predictions are consistent with biophysical measurements of nearly additive mutational effects on stability [18], and with reports of consistent effects over both short [14] and long [19] evolutionary timescales. And yet, at the same time, we show that a non-additive contribution to the folding free energy is essential for allowing proteins to fold stably in our model, for reasons attributable to sequence entropy. These results may help to resolve striking discrepancies in the literature on the importance of epistasis for protein stability and evolution [1–5].

2. Methods

2.1. Simulations

We consider two simple models for the relationship between amino acid sequences and ΔG of folding. All amino acid sequences considered are of length $l = 400$.

First we consider a model where epistasis arises due to pair-wise interactions between sites. In this probabilistic model, the additive effect on stability for each possible amino acid in each position in the primary sequence is drawn from a Gaussian distribution with mean μ_{add} and variance σ^2_{add}. In addition, we allow pair-wise interactions between amino acid sites, and the magnitudes of these interactions are also drawn from a Gaussian distribution with zero mean and variance σ^2_{epi}. Moreover, these pairwise interactions are specified in such a way that the pairwise interaction terms have no impact on the average effect of any given amino acid substitution, so that the magnitudes of the additive and epistatic effects can be modified independently. That is, the model is equivalent to a "random field model" from the fitness landscape literature[20,21] where the only non-zero terms are the constant, linear, and pairwise interaction terms. See Appendix A for details on the mathematical features and practical implementation of this model.

Second, we consider a model where epistasis is modeled as a random deviation from additivity drawn independently for each *genotype*, meaning each sequence of amino acids. This model is similar to the "rough Mount Fuji" model of fitness landscapes [22,23]. In this case we again draw the additive effect of each amino acid in each position from a Gaussian distribution with variance σ^2_{add}, but in addition the folding energy of each genotype is perturbed by an independent draw from a zero-mean gaussian with variance σ^2_{HOC} (where *HOC* denotes "house of cards", since this component is completely uncorrelated between mutationally adjacent genotypes, similar to the house of cards model of fitness landscapes [24]). Because protein sequence space is too large to store in computer memory, we implement a hashing scheme so that in the simulations these epistatic effects remain consistent for previously observed genotypes, but are drawn anew for genotypes that have not yet been encountered.

The simulations of protein sequence evolution under selection are based on a threshold model for thermodynamic stability: proteins with a negative ΔG of folding are deemed viable and all other sequences are deemed inviable. At each step in the simulation, a random position in the protein

sequence is chosen and changed to a random alternative amino acid. This new sequence is accepted if it is viable and rejected if it is inviable. These simulations are initialized at the sequence predicted to be most stable based on its additive effects and allowed to equilibrate for 5000 proposed mutations, a time sufficient for the distribution of folding stabilities to become approximately stationary for the conditions consider here. After this relaxation period, the simulations continue for an additional 5000 proposed mutations to produce the results shown here. All simulations and all calculations presented were implemented in Mathematica and the corresponding Mathematica notebook is included as supplemental information.

The models analyzed here are simpler, and less realistic, than other commonly used models for protein evolution based on force fields [25], contact energies [26], or lattice proteins [27]. However, we employ these models because their simple structure yields to a variety of exact and approximate analytical results, and thus provides a clearer illumination of the theoretical issues involved than the more realistic but less tractable alternatives.

3. Results

3.1. Epistasis is essential for proper folding of evolved sequences

We simulated the evolution of a protein of length 400 under a model where each amino acid at each position makes an additive contribution to the free energy of folding, and where in addition we allow pairwise stability interactions between sites. We imposed truncation selection for spontaneous folding so that only sequences with a negative ΔG of folding are considered viable. The parameters of the simulations were chosen to be roughly consistent with the observed distribution of folding stabilities and mutational effects on stability reported in the literature [e.g. 28–31]

Figure 1a shows the distribution of folding energies observed in these simulations after the process was allowed to reach stationarity. The mean of this distribution is only slightly negative, indicating that the evolved proteins are marginally stable, as predicted by theory and observed in nature [8,11,29,31,32]. Examining the effects of single amino acid substitutions for sequences drawn from this distribution (Figure 1b), we observe that the mean is approximately positive 1.133 kcal/mol with standard deviation 1.44 kcal/mol, consistent with empirical observations [28–30], and that the distribution of energetic effects that are fixed over the course of the simulations (Figure 1c) is shifted to have approximately zero mean (0.0009 kcal/mol) and a smaller standard deviation (1.0493 kcal/mol) as observed previously [16,33,34].

Interactions between mutations also have a similar magnitude to those observed in previous studies, with double mutants stabilities nearly exactly predicted by the observed additive effects of their constituent single mutations (Figure 1d, $R^2 = 0.99976$). Furthermore, the additive effects of mutations that fix along our simulated evolutionary trajectories remain relatively consistent over time (Figure 1e), with a root mean square change of only 0.5052 kcal/mol at 50% sequence divergence, consistent with the empirical measurements of Risso *et al.* [19], who observed an RMS change of .67 kcal/mol among mutations that fix at a similar level of divergence. Because we are working with simulated data, we can also assess the extent to which the observed mutational effects reflect the true additive effects of mutations. Figure 1f shoes that the observed effects of the possible single amino acid substitutions in an evolved background are highly correlated with the true underlying additive effects of these same mutations ($R^2 = 0.887$).

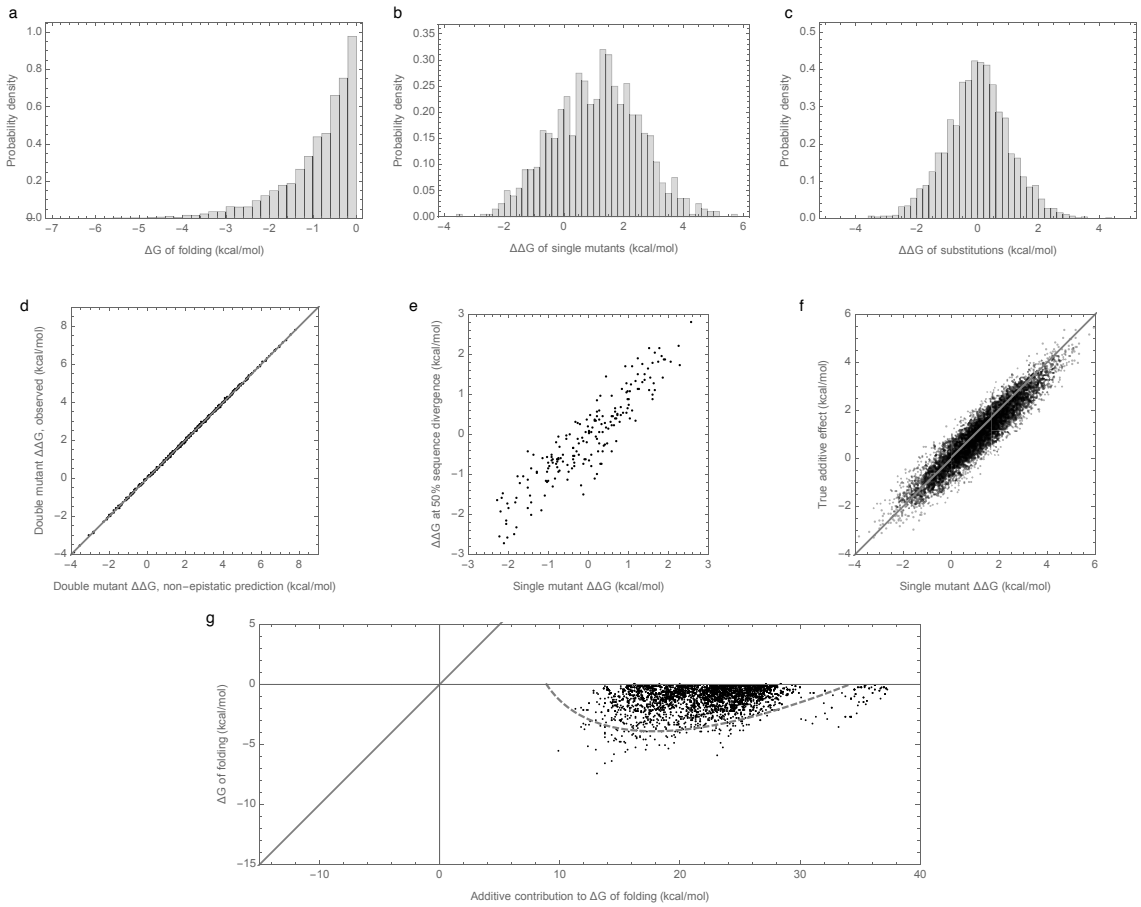

Figure 1. Free energy of folding, stability effects of mutations, and contribution of additive effects to folding stability for populations evolving at stationarity under truncation selection for protein stability with pair-wise energetic interactions: (**a**) Free energy of folding for evolved sequences. (**b**) Distribution of stability effects of mutations for evolved sequences. (**c**) Distribution of stability effects of mutations fixed along simulated trajectories. (**d**) Stability effects of double mutants for evolved sequences versus predicted stability based on the sum of single mutant effects. 500 random double mutants in a single evolved background shown, $R^2 = 0.99976$. (**e**) Effects of single mutations that fixed along trajectory in two evolved backgrounds that differ by 50% sequence divergence, $R^2 = 0.8266$. (**f**) Observed stability effects of mutations are highly correlated with the true average additive effects of the corresponding mutations, $R^2 = 0.887$. (**g**) Free energy of folding versus additive contribution to folding for evolved sequences. The additive contribution to folding is not a good indicator of the free energy of folding ($R^2 = 0.0672$) and observed sequences cannot fold spontaneously based on the additive contribution alone. The solid curve is derived from our analytical approximations and is predicted to contain 95% of the evolved sequences. Simulations conducted under the pairwise epistasis model with $\mu_{\text{add}} = 1$, $\sigma^2_{\text{add}} = 1$, $\sigma^2_{\text{epi}} = 0.0003$.

To summarize, our simulations are qualitatively similar to both previous empirical and theoretical investigations of long-term evolution under selection for protein folding stability, and, on the face of it, they suggest that epistasis for protein folding stability plays only a minor role. However, when we actually compute the additive contribution to protein stability observed in our simulations, a very different picture emerges (Figure 1d). Shockingly, we find that the observed additive contribution to folding stability is not nearly sufficient to allow spontaneous folding (mean ΔG of folding from the additive component is 22.45 kcal/mol) so that epistatic interactions are required for folding for all the sequences observed at stationarity. Furthermore, the additive contribution to folding stability is almost completely uncorrelated with the actual folding stability (R^2=0.06). Thus, epistasis plays an essential

role in the simulation results, despite its near absence in the simulated double-mutant data and the observed conservation of energetic effects at 50% sequence divergence.

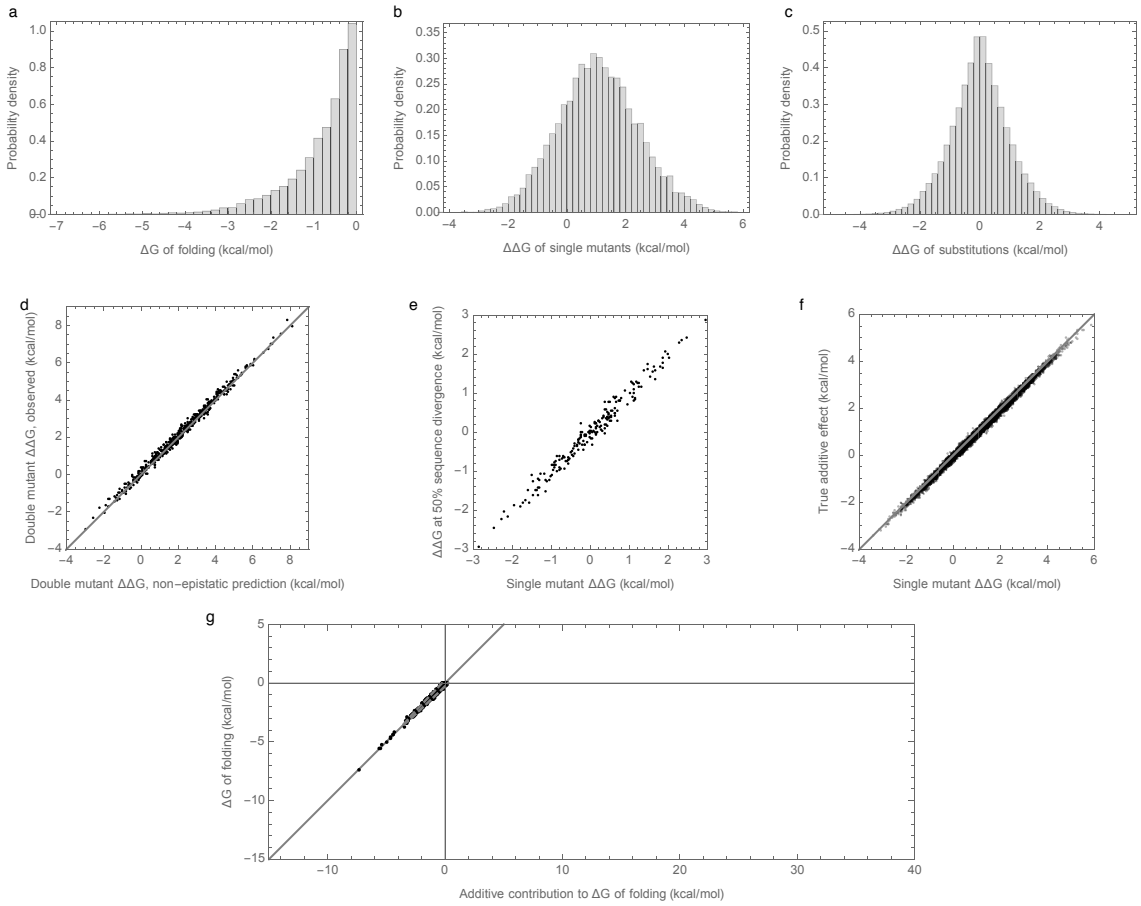

Figure 2. Free energy of folding, stability effects of mutations, and contribution of additive effects to folding stability for populations evolving at stationarity under truncation selection for protein stability under the independent epistatic effects model: (**a**) Free energy of folding for evolved sequences. (**b**) Distribution of stability effects of mutations for evolved sequences. (**c**) Distribution of stability effects of mutations fixed along simulated trajectories. (**d**) Stability effects of double mutants for evolved sequences versus predicted stability based on the sum of single mutant effects. 500 random double mutants are shown. (**e**) Effects of single mutations that fixed along trajectory in two evolved backgrounds that differ by 50% sequence divergence, $R^2 = 0.9856$. (**f**) Observed stability effects of mutations are highly correlated with the true average additive effects of the corresponding mutations. (**g**) The additive contribution to folding is a good indicator of the free energy of folding ($R^2 = 0.9863$) and 95% of observed sequences can fold spontaneously based on the additive contribution alone. The solid curve is derived from our analytical approximations and is predicted to contain 95% of the evolved sequences. Simulations conducted under the independent random effects model with $\mu_{\text{add}} = 1, \sigma^2_{\text{add}} = 1, \sigma^2_{\text{HOC}} = .01$.

3.2. Enrichment for epistasis observed under pairwise, but not independent models

In order to better understand the causes of these counter-intuitive results, we considered an alternative landscape with an identical additive component but with epistasis modeled as random draw for each sequence (from a zero-mean Gaussian distribution with variance $\sigma^2_{\text{HOC}} = .01$), Figure 1c. The results of these simulations are shown in Figure 2. In this case, the distribution of folding stabilities, distribution of mutational effects, and extent of observed epistasis in pairwise mutations are qualitatively unchanged from the results observed under the prior, pairwise interaction model

(Figure 2a-f vs. Figure 1a-f). However, in this case the paradoxical contribution of epistasis to folding stability is absent, so that the additive contribution to stability is sufficient for spontaneous folding for most evolved sequences, and the observed folding energy is highly correlated with the additive contribution (R^2=0.9865, Figure 2d). We therefore conclude that enrichment for epistasis under stabilizing selection occurs with pair-wise epistatic interactions but not with fully random interactions.

What explains this difference in behavior between the model with pair-wise epistatic interactions and the model with independent epistatic effects for each sequence? In order to address this question, we conducted a mathematical analysis of the random field model (see Appendix B). What we came to understand was that the amount of epistasis observed in double mutants under the pair-wise interaction model vastly underestimates the total amount of epistasis in the energy landscape. This occurs because making a double mutant only results in changes to relatively few interaction pairs (i.e. those interaction pairs involving the site of either single mutant). However, as additional mutations are added to the sequence, more pairs are perturbed, which unleashes additional epistasis.

More precisely, in the mathematical analysis we considered the expected magnitude of the observed epistasis as a function of the number of mutations from an arbitrary focal sequence. That is, we calculated the expected variance in the epistatic contribution among the set of all sequences at a given distance d from this focal sequence. The results are shown in Figure 3 where the variance at $d = 2$ is set to 1, so that the variance is expressed relative to the variance observed in a double mutant analysis. We see that for small d this variance increases roughly linearly, and eventually saturates at almost 50 times the expected variance at $d = 2$. In contrast, the independent random epistasis model is essentially constant at all positive distances. Thus, similar levels of observed epistasis in double mutants make vastly different predictions for the total amount of epistasis under the two models.

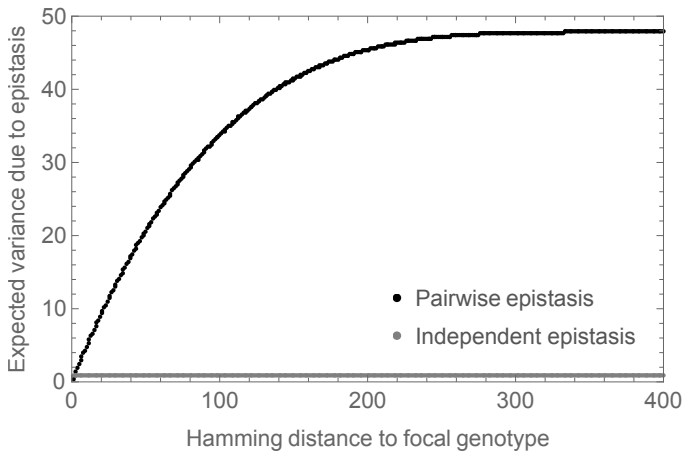

Figure 3. Expected epistatic variance as a function of distance from the focal sequence for amino acid sequences of length $l = 400$. Results for the pair-wise model shown in black, results for the independent epistasis model shown in gray. All variances are normalized relative to the expected variance at $d = 2$ which is set to 1. Notice that epistatic variance at large distances is much larger than epistatic variance at distance $d = 2$ for the pair-wise epistasis model but not for the independent epistasis model.

3.3. Bivariate normal approximation for joint distribution of additive and epistatic contributions captures impact of sequence entropy

Our results on the surprising implications of small observed epistatic effects under the pairwise interaction model make the results in Figure 1g appear somewhat more plausible because more epistasis is present in the landscape than is apparent from the double mutants. But this observation still does not provide a definite explanation for the large contribution of epistatic interactions to folding stability.

We now provide such an explanation, based on considering the fraction of random sequences that have any given pair of additive and epistatic contributions (see Appendix C for details). In particular, we assume that the distribution of additive contributions to the free energy of folding for random sequences is normally distributed with mean μ_1 and variance σ_1^2, that the distribution of epistatic contributions is normally distributed with mean 0 and variance σ_2^2, and that the additive and epistatic contributions are uncorrelated so that the total folding energy of a random sequence $\Delta G = \Delta G_{\text{add}} + \Delta G_{\text{epi}}$ is also normally distributed, with mean $\mu = \mu_1$ and variance $\sigma^2 = \sigma_1^2 + \sigma_2^2$. These normal approximations are reasonable considering that ΔG_{add} is calculated by adding up the energy contribution of each site in the sequence, and ΔG_{epi} is calculated by adding up the energy contribution of each pair of sites in the sequence for a large number $l = 400$ of sites. We also note that in the mutation-limited regime depicted in our simulations, the stationary distribution of the simulated random walk will be uniform on the set of genotypes with negative folding energies that are path-connected with our choice of starting genotype [35]. Under the assumption that almost all genotypes with negative folding energies are path-connected, picking a sequence from the stationary distribution is equivalent to picking a sequence from the uniform distribution on sequences with negative folding energies, and so our problem reduces to understanding the distribution of additive folding contributions among all sequences with negative free energies of folding.

Under the above approximation, we now consider how—for a typical viable sequence— the additive and epistatic energies jointly produce a negative free energy of folding. The key idea is that there are so many more sequences with positive additive contributions to folding than there are sequences with negative additive contributions that most sequences that fold have a positive additive contribution despite the fact that any particular sequence with a positive additive contribution to the free energy of folding has only a minuscule chance of actually folding.

More precisely, let us fix the value of the additive energy at $\Delta G_{\text{add}} = x$, and count the number of sequences, with this given ΔG_{add}, that fold. The number of sequences with $\Delta G_{\text{add}} = x$ is proportional to the probability density for the distribution of ΔG_{add}, $\text{PDF}(\mathcal{N}(\mu_1, \sigma_1^2))(x)$. Adding the epistatic energy to the additive energy, the sequences with $\Delta G_{\text{add}} = x$ that fold are the sequences for which $\Delta G_{\text{epi}} < -x$, i.e. their number is proportional to the cumulative distribution function of ΔG_{epi} evaluated at $-x$, $\text{CDF}(\mathcal{N}(0, \sigma_2^2))(-x)$. Putting the two pieces together, the number of sequences that have $\Delta G_{\text{add}} = x$ and, at the same time fold, is proportional to

$$\text{PDF}(\mathcal{N}(\mu_1, \sigma_1^2))(x) \times \text{CDF}(\mathcal{N}(0, \sigma_2^2))(-x).$$

Figure 4 shows this calculation for x values near the viability threshold 0. We see that over this range of folding energies the number of sequences is growing extremely rapidly (Figure 4a) so that, roughly speaking, the number of sequences with a given additive energy increases 10-fold for every additional .45 kcal/mol. Now, Figure 4b shows the fraction of sequences with a given additive contribution that spontaneously fold. This is near 1 for most sequences with a negative contribution, but decreases exponentially for positive additive contributions. The net result (Figure 4c) is that a typical additive contribution for a sequence that folds is often around 22 or 23 kcal/mol. While only a tiny fraction of sequences with additive energies in this range fold (roughly 1 in a million), there are roughly 10 billion times more sequences in this 1 kcal/mol range than there are all sequences that would spontaneously fold based on their additive contribution (i.e. with $\Delta G_{\text{add}} < 0$), so that in the end most sequences that fold have substantially positive additive contributions to the free energy of folding.

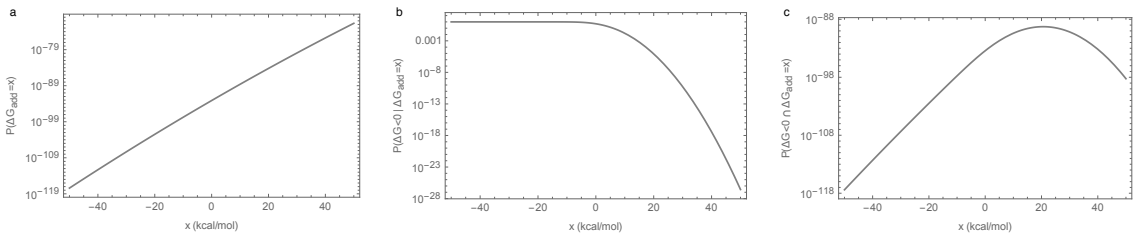

Figure 4. Illustration of the main mechanism behind the essentiality of epistatic interactions for spontaneous folding: (**a**) Density of random sequences with given additive free energy $\mathrm{P}\left(\Delta\mathrm{G}_{\mathrm{add}} = x\right) = \mathrm{PDF}(\mathcal{N}(\mu_1, \sigma_1^2))(x)$. (**b**) Fraction of sequences that fold given additive free energy $P(\Delta\mathrm{G} < 0 | \Delta\mathrm{G}_{\mathrm{add}} = x) = \mathrm{CDF}(\mathcal{N}(0, \sigma_2^2))(-x)$. (**c**) Density of random sequences that fold and have the given additive free energy $\mathrm{P}\left(\Delta\mathrm{G} < 0 \cap \Delta\mathrm{G}_{\mathrm{add}} = x\right)$.

The above argument leads to a simple prediction for the joint distribution of the free energy of folding and additive contribution to folding shown in Figures 1g and 2g: since the joint distribution for random sequences is bivariate normal, the distribution of observed energies should simply be this bivariate normal distribution truncated at $\Delta\mathrm{G} = 0$ kcal/mol. This approximation is shown in Figures 1g and 2g by a dashed gray curve that is predicted to contain 95% of the observations, and we see that this prediction is in reasonable agreement with our simulations.

Moreover, under this bivariate normal approximation the average contribution of epistasis to the mean free energy of folding observed in our simulations can be calculated in a manner exactly analogous to Galton's classical results on regression to the mean [36], or the difference between the selection differential and the response to selection in the breeder's equation from quantitative genetics [37,38]. In particular, we find that the mean additive energy of viable sequences is approximately $E(\Delta G_{\mathrm{add}} | \Delta G < 0) \approx \mu\sigma_2^2/(\sigma_1^2 + \sigma_2^2)$ (see Appendix C for details), so that the mean contribution of epistasis is approximately $-\mu\sigma_2^2/(\sigma_1^2 + \sigma_2^2)$, or equivalently $-\mu(1 - R^2)$, where R^2 is given by the squared correlation coefficient of additive and total folding energies taken over all of sequence space. As a result, even if the mapping from sequence to folding energy is nearly additive, in the sense that R^2 is almost 1, the predicted epistatic contribution to the folding stability can still be substantial provided that the expected folding energy μ of a random sequence is sufficiently disfavorable.

4. Discussion

The role of epistasis in long-term protein evolution remains a topic of active debate [1–5]. Here we have explored a surprising phenomenon where the effects of mutations on the ΔG of folding appear to combine nearly additively, and nonetheless what little epistasis is present plays a critical role, to the extent that observed sequences would not be able to fold in the absence of these epistatic interactions. We showed that this phenomenon occurs in a model where interactions occur between pairs of sites but not in a model where each sequence differs from its additive prediction by an independent draw from a normal distribution. The difference between the two models arises because pair-wise interactions can appear nearly additive in double mutants while still producing a substantial amount of epistasis over sequence space as a whole. We also present simple analytical approximations that predict the extent of the epistatic contribution to stability in our simulations. Furthermore, these approximations suggest that this phenomenon occurs due to sequence entropy: many more sequences can fold due to a combination of epistatic and additive contributions than can fold based on the additive contributions to stability alone, and so the epistatic contribution to stability is typically essential when one observes a random sequence that folds. These results add to a growing literature demonstrating that natural selection can enrich for epistatic interactions in both adaptive [39–41], and nearly neutral [16] evolution, such that the mutations that fix during evolution can have a very different pattern of epistasis than random mutations.

Our simulations (Figure 1) recapitulate the known qualitative features of protein evolution under purifying selection for folding stability to a surprising degree, with the exception of matching the observed stability margin, which is smaller in our simulations than for experimentally measured folding energies [29] (free energy of folding is typically -5 to -10 kcal/mol versus -1 kcal/mol in our simulations). However, this extremely small stability margin is a well-known artifact of our decision to model fitness as a step function in stability [8] rather than a more realistic logistic function [11,30], and the fact that our simulations do not include any of the other factors that would tend to increase the stability margin such as selection for mutational robustness [8,32,35] or selection to prevent misfolding due to errors in translation [42]. Nonetheless the simple sequence-to-fitness mapping employed in our simulations allows us to provide a relatively simple and complete theory for the observed phenomenon. Moreover, we emphasize that it is easy to find realistic parameters where the mean additive contribution to stability is far less stable than shown in Figure 1, so we anticipate that the possibility that most sequences fold only due to epistasis would be robust even if sequences experienced a much larger stability margin.

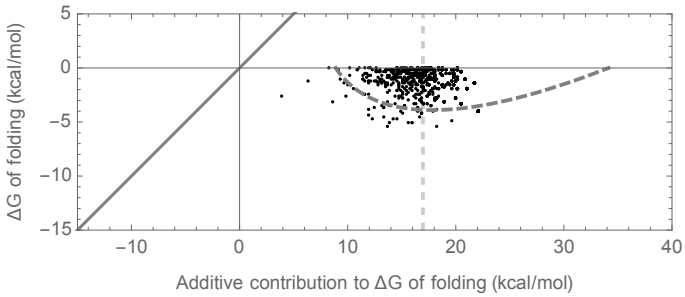

Figure 5. Joint distribution of ΔG of folding and the additive contribution to ΔG of folding for the independent epistasis model with σ^2_{HOC} chosen so that the bivariate normal approximation matches the bivariate normal approximation shown in Figure 1g. Simulations conducted under the independent epistasis model with $\mu_{\mathrm{add}} = 1$, $\sigma^2_{\mathrm{add}} = 1$, $\sigma^2_{\mathrm{HOC}} = 21.6$. Dashed curve shows area predicted to include 95% of sequences at stationarity under the bivariate normal approximation; dashed vertical line shows approximate left-most edge of region where bivariate normal approximation is valid based on a crude percolation theory argument (see text).

A different limitation of our results concerns the assumption, in our truncated bivariate normal approximation, that the set of sequences with negative folding energies is mutationally connected, and hence accessible to an evolving population. In particular, the theory breaks down if a large fraction of sequences that fold appear as isolated peaks or small isolated clusters of sequences. Figure 5 shows an example of this limitation for the case of the independent model with parameters chosen so that the bivariate normal approximation is identical to the bivariate normal approximation for the pairwise model shown in Figure 1. The figure shows some enrichment for epistasis but not as much as predicted by our bivariate normal approximation. Using the crude percolation-theory argument that the connected network of sequences can extend only up to the additive energy at which each sequence has on average one neighbor that folds due to epistasis [43], we can derive the approximate upper limit of the distribution of additive energies as $-\sigma_{\mathrm{HOC}}\Psi^{-1}(1/(400 \times 19)) = 16.96$, where Ψ^{-1} is the inverse cumulative distribution function of a standard normal distribution. This approximate upper limit is shown by the dashed vertical line in Figure 5. We see that the cloud of observed sequences is primarily to the left of this line, with a notable absence of sequences with substantially more positive additive contributions. This analysis of connectivity of the set of sequences that fold highlights that pairwise interactions have several special features: not only can they appear locally non-epistatic while harboring a substantial amount of epistasis at greater distances, but as long as the individual coefficients remain small they produce energy landscapes that change smoothly over sequence space,

producing the enormous connected networks of sequences whose traversal allows the evolution of a sizable epistatic contribution to folding.

It is natural to ask whether the essentiality of epistatic interactions for the functionality of evolved sequences is likely to hold in other contexts where additivity is thought to prevail, such as protein-DNA and protein-protein binding [18]. However, this effect is unlikely to occur in most of these cases because the sequences are much shorter and the set of functional sequences makes up a much larger proportion of genotypic space. In particular, it is helpful to consider the z-score of functional sequences relative to random sequences, since the regression to the mean effect observed here is proportional to the absolute value of the z-score. For instance, the average TF binding motif in bacteria has an information content of 23 bits, corresponding to a p-value of 10^{-7} or a z-score of roughly -5, with eukaryotic transcription factors having even smaller information contents and therefore smaller absolute value z-scores [44]. In contrast, the z-scores of the spontaneously folding sequences observed in our simulations are on the order of -20, which we would expect to result in a roughly 4-fold larger contribution of epistasis to binding energy at stationarity than for a bacterial transcription factor binding site. Such extreme z-scores are not even possible in short DNA elements, e.g. the most extreme z-score possible in a DNA sequence of length 20 is only -7. Thus, the essentiality of epistatic interactions observed here is likely possible only because protein sequence space is very large compared to other well-studied sequence-function relationships focused on smaller genetic elements.

Finally it is important to emphasize that the key question of whether epistatic interactions for protein stability are essential for protein folding in naturally evolved sequences remains open. Our contribution only demonstrates that such an effect is qualitatively consistent with empirical observations on the thermodynamic effects of mutations and the results of prior simulation studies, and suggests that the overall importance of epistasis for stability depends on the precise form of epistasis involved. Intriguingly, the experimental observation that pairwise correlations between site-specific amino acid usages are sometimes necessary for folding [45] provides evidence for both the presence of the low-order epistatic interactions that result in a substantial contribution of epistasis to protein folding and also for the possible essentiality of these interactions. Thus, determining whether epistasis is essential for folding of observed sequences is a key question for the field, from both theoretical and empirical perspectives. Importantly, our analysis shows that most standard designs for examining the extent of epistasis for protein stability cannot adjudicate this question, because they examine how the extent of mutations change at a only single distance from a reference genotype. For instance, the analysis of double mutants considers the change in the effect of a mutation in a sequence at distance 1; and comparison of the effects of mutations on two diverged backgrounds, e.g., [14,19], can only determine the extent of epistasis at that one level of divergence. Rather, the two theories analyzed here differ in how the extent of epistasis changes with distance (e.g. Figure 3 and Appendix B.3). Thus, the critical experiment is to measure how the energetic effects of individual mutations change across several different levels of sequence divergence (c.f. [16]).

Author Contributions: Conceptualization, A.P., J.B.P, J.B.K., and D.M.M.; Software, A.P., J.Z., and D.M.M.; Formal Analysis A.P., J.Z., J.B.K. and D.M.M.; Investigation A.P. and D.M.M.; Writing - Original Draft Preparation, A.P., J.Z., J.B.P, J.B.K., and D.M.M.; Writing - Review & Editing, A.P., J.B.P. and D.M.M.; Funding Acquisition, J.B.P and J.B.K.

Funding: J.B.K. and A.P. were supported in part by a grant from the CSHL/Northwell Health alliance. J.B.P. acknowledges support from the David and Lucile Packard Foundation and the U.S. Army Research Office (W911NF-12-R-0012-04).

Acknowledgments: We thank Ashley Teufel and David Liberles for organizing this special issue of Genes.

Conflicts of Interest: The authors declare no conflict of interest. The founding sponsors had no role in the design of the study; in the collection, analyses, or interpretation of data; in the writing of the manuscript, and in the decision to publish the results.

Appendix A

Appendix A.1 Model for folding energy

Given an alphabet $\mathcal{A} = \{0, 1, ..., a-1\}$ and a sequence length l, let $\mathcal{S}$ be the set all possible strings of length l built from alphabet $\mathcal{A}$. The free energy of folding $\Delta G(x)$ for each sequence $x \in \mathcal{S}$ is defined as the sum of (1) an additive component that measures the energy contribution of each allele at each position in the sequence, and (2) an epistatic component that describes the energy contribution of pairwise interactions among alleles for the pairwise model, or a random draw from a normal distribution for the independent epistasis model:

$$\Delta G(x) := \Delta G_{\text{add}}(x) + \Delta G_{\text{epi}}(x). \tag{A1}$$

To specify each of the terms $\Delta G_{\text{add}}(x)$ and $\Delta G_{\text{epi}}(x)$, we introduce the following notations. Let x_k denote the k-th letter in the sequence x. Then, for a set of indices $K = \{k_1, \ldots, k_{|K|}\}$, let $\beta_{K,\alpha}$ denote the energetic contribution to the folding energy of x when the substring $x_{k_1} x_{k_2} \ldots x_{k_{|K|}}$ is equal to α. Using this notation, we let:

$$\Delta G_{\text{add}}(x) := \sum_{k=1}^{l} \beta_{\{k\},x_k} \tag{A2}$$

be the additive contribution to the folding energy, and

$$\Delta G_{\text{epi}}(x) := \sum_{k_1=1}^{l-1} \sum_{k_2=k_1+1}^{l} \beta_{\{k_1,k_2\},x_{k_1}x_{k_2}} \tag{A3}$$

be the epistatic contribution for the pairwise model. For the independent epistasis model, we instead let $\Delta G_{\text{epi}}(x)$ be an independent random draw from a normal distribution with mean 0 and variance σ^2_{HOC}.

Having described the form of our energy model, we now describe how we choose the $\beta_{K,\alpha}$. Some care is needed in this choice in order to ensure that $\Delta G_{\text{epi}}(x)$ for the pairwise model is a pure epistatic contribution, that is, that the average effect of any given point mutation over sequence space is zero. For the independent epistasis model, no additional steps are needed because the epistatic contribution is drawn independently for each sequence and each possible point mutation can appear on many genetic backgrounds, so by the law of large numbers the average epistatic effect of any given point mutation will be very near zero.

We first describe how we choose the $\beta_{K,\alpha}$ for the additive component. For each position k, the vector of coefficients $\vec{\beta}_{\{k\}} := (\beta_{\{k\},0}, \ldots, \beta_{\{k\},\alpha-1})$ specifies the contribution to folding energy of each allele at the given position. We impose the constraint

$$\frac{1}{a} \sum_{\alpha=0}^{a-1} \beta_{\{k\},\alpha} = \mu_{\text{add}}, \tag{A4}$$

so that the mean additive folding energy over all possible sequences is $l\mu_{\text{add}}$, i.e. $\langle \Delta G_{\text{add}}(x) \rangle_x = l\mu_{\text{add}}$.

Turning to the epistatic component for the pair-wise model, for each position pair (k_1, k_2) such that $k_2 < k_1$, the matrix of coefficients $B_{\{k_1,k_2\}} := (\beta_{\{k_1,k_2\},\alpha_1\alpha_2})_{\alpha_1\alpha_2}$ specifies the contribution to folding energy resulting from the interaction of the alleles at the given positions. We impose the constraints that all row and all column sums of $B_{\{k_1,k_2\}}$ equal 0, i.e.

$$\sum_{\alpha_1=0}^{a-1} \beta_{\{k_1,k_2\},\alpha_1\alpha_2} = 0,\ \alpha_2 \in \mathcal{A}, \quad \text{and} \quad \sum_{\alpha_2=0}^{a-1} \beta_{\{k_1,k_2\},\alpha_1\alpha_2} = 0,\ \alpha_1 \in \mathcal{A}. \tag{A5}$$

These constraints ensure that the mean epistatic energy over all possible sequences is 0, i.e. $\langle \Delta G_{\text{epi}}(x) \rangle_x = 0$. It also follows from conditions (A4) and (A5) that the vectors $\Delta G_{\text{add}} := (\Delta G_{\text{add}}(x))_{x \in \mathcal{S}}$ and $\Delta G_{\text{epi}} := (\Delta G_{\text{epi}}(x))_{x \in \mathcal{S}}$ are orthogonal, see Appendix B.2.

We now turn to our procedure for drawing the additive and pairwise coefficients $\beta_{K,\alpha}$ subject to the above constraints.

Appendix A.2 Choosing the coefficients for the energy function

For each position k, we choose $\vec{\beta}_{\{k\}} := (\beta_{\{k\},0}, \ldots, \beta_{\{k\},a-1})$ from an a-dimensional normal distribution that has identical marginals, mean vector $(\mu_{\text{add}}, \ldots, \mu_{\text{add}})$, and some covariance matrix that ensures that constraint (A4) is satisfied. Similarly, for each pair of positions (k_1, k_2), $k_2 < k_1$, we choose the elements of $B_{\{k_1,k_2\}} := (\beta_{\{k_1,k_2\},\alpha_1\alpha_2})_{\alpha_1\alpha_2}$ from an a^2-dimensional normal distribution that has identical marginals, mean vector $\vec{0}$, and some covariance matrix that ensures that the constraints in (A5) are satisfied. To draw the coefficients from such distributions we implement the following procedures.

Appendix A.2.1 Choosing the coefficients for the first order terms

The subspace of $\mathbb{R}^a$ defined by the constraint in (A4) is a hyperplane specified by the normal vector $\vec{n} = (1, \ldots, 1)$ going through the point $(\mu_{\text{add}}, \ldots, \mu_{\text{add}})$. Let $\vec{e}_i$, $i = 1, \ldots, a$, denote the standard basis in $\mathbb{R}^a$, i.e. $(\vec{e}_i)_j = 1$ if $j = i$ and 0 otherwise. We obtain a basis spanning $\mathbb{R}^a$ if we take the standard basis and replace its first vector by $\vec{n}$:

$$\{\vec{n}, \vec{e}_2, \ldots, \vec{e}_a\}.$$

By performing Gram-Schmidt orthogonalization on this set of vectors, in the given order, we obtain an orthogonal basis in $\mathbb{R}^a$ whose first vector is the normal vector $\vec{n}$. Let $\vec{b}_i$, $i = 1, \ldots, a-1$, denote the normalized vectors of this basis other than $\vec{n}$, i.e. the $\vec{b}_i$ vectors are orthonormal and span the hyperplane specified by constraint (A4). It follows that if $\vec{z} \in \mathbb{R}^{(a-1)}$ is a vector of iid random variables of normal distribution with mean 0 and some standard deviation σ_{add}, then the vector

$$(\mu_{\text{add}}, \ldots, \mu_{\text{add}}) + \sum_{k=1}^{a-1} z_k \vec{b}_k \tag{A6}$$

has the desired distribution. In particular, each component $\mu_{\text{add}} + \sum_{k=1}^{a-1} z_k (\vec{b}_k)_i$ has normal distribution with mean μ_{add} and variance $((\alpha - 1)/\alpha)\sigma^2_{\text{add}}$, i.e.

$$\beta_{\{k\},\alpha} \sim \mathcal{N}\left(\mu_{\text{add}}, \sqrt{\frac{\alpha - 1}{\alpha}}\sigma_{\text{add}}\right). \tag{A7}$$

Appendix A.2.2 Choosing the coefficients for the second order terms

For each position pair (k_1, k_2), $k_2 < k_1$, we choose the elements of $B := (\beta_{\{k_1,k_2\},\alpha_1\alpha_2})_{\alpha_1\alpha_2}$ from an a^2-dimensional normal distribution that has identical marginals, mean vector $\vec{0}$, and some covariance matrix that ensures that the constraints in (A5) are satisfied. In what follows, instead of using the matrix notation B for the coefficients, we use a vector notation, obtained by concatenating the rows of B.

The subspace of $\mathbb{R}^{a^2}$ defined by the constraints in (A5) is obtained as the intersection of the set of hyperplanes specified by the normal vectors

$$(\vec{n}_{\text{row,i}})_j = \begin{cases} 1 & \text{if } j \in \{(i-1)a + 1, (i-1)a + 2, \ldots, (i-1)a + (a-1)\} \\ 0 & \text{otherwise} \end{cases}, \quad i = 1, 2, \ldots, a-1, \tag{A8}$$

$$(\vec{n}_{\text{column},i})_j = \begin{cases} 1 & \text{if } j \in \{i, a+i, 2a+i, \ldots, (a-2)a+i\} \\ 0 & \text{otherwise} \end{cases}, \quad i = 1, 2, \ldots, a-1, \tag{A9}$$

and

$$\vec{n}_j = 1, \quad j \in \{1, 2, \ldots, a^2\}. \tag{A10}$$

Let $\vec{e}_i$, $i = 1, \ldots, a^2$, denote the standard basis in $\mathbb{R}^{a^2}$, i.e. $(\vec{e}_i)_j = 1$ if $j = i$ and 0 otherwise. Then, the set of vectors

$$\{\vec{n}\} \cup \{\vec{n}_{\text{row,i}} : i = 1, \ldots, a-1\} \cup \{\vec{n}_{\text{column,i}} : i = 1, \ldots, a-1\} \cup \{\vec{e}_i : i = 1, \ldots, (a-1)^2\}$$

form a basis spanning $\mathbb{R}^{a^2}$. By performing Gram-Schmidt orthogonalization on this set of vectors, in the given order, we obtain an orthogonal basis in $\mathbb{R}^{a^2}$ whose first $2a-1$ vectors span the orthogonal complement of the subspace defined by the constraints in (A4). Let us denote the normalized version of the rest of the vectors of this basis by $\vec{b}_i$, $i = 1, \ldots, (a-1)^2$. If $\vec{z} \in \mathbb{R}^{(a-1)^2}$ is a vector of iid random variables of normal distribution with mean 0 and some standard deviation $\sigma_{\beta,2}$, then the vector

$$\sum_{k=1}^{(a-1)^2} z_k \vec{b}_k \tag{A11}$$

has the desired distribution. In particular, each component $\sum_{k=1}^{(a-1)^2} z_k (\vec{b}_k)_i$ has normal distribution with mean 0 and variance $(\alpha-1)^2/\alpha^2 \sigma^2_{\text{add}}$, i.e.

$$\beta_{\{k_1,k_2\},\alpha_1\alpha_2} \sim \mathcal{N}\left(0, \frac{\alpha-1}{\alpha}\sigma_{\text{epi}}\right). \tag{A12}$$

Appendix B

Appendix B.1 Background

To derive the expected variance due to epistasis at a given distance from a focal genotypes, as shown in Figure 3, we will first need to introduce some notation .

Given an alphabet $\mathcal{A} = \{0, 1, ..., a-1\}$, let $\mathcal{S}$ be the set all possible sequences (configurations) of length l, with cardinality $|\mathcal{S}| = a^l \equiv N$. We introduce the Hamming distance $\mathbf{d}$:

$$\mathbf{d} : \mathcal{S} \times \mathcal{S} \to \{0, 1, \cdots, l\}$$

$$\mathbf{d}(x, x') = \mathbf{d}(x', x) = \text{Number of sites where } x \text{ and } x' \text{ differ.}$$

Then set of all sequences form the Hamming graph, $\mathcal{G} = (\mathcal{S}, E)$, with set of edges

$$E = \{(x, x') \in \mathcal{S} \times \mathcal{S} | \mathbf{d}(x, x') = 1\}$$

That is, two sequences x and x' are adjacent on $\mathcal{G}$, i.e. $x \sim x'$, if and only if $\mathbf{d}(x, x') = 1$.

The graph Laplacian L of $\mathcal{G}$ is a $N \times N$ matrix

$$L(x, x') = \begin{cases} l(a-1) & x = x' \\ -1 & x \sim x' \\ 0 & \text{otherwise} \end{cases}. \tag{A13}$$

Applying L to any N-dimensional vector f, we have

$$(Lf)(x) = l(a-1)f(x) - \sum_{x' \sim x} f(x') = \sum_{x' \sim x} f(x) - f(x'), \tag{A14}$$

which is the sum of differences between the focal type x and all the adjacent sequences.

The graph Lalpacian L has $l+1$ distinct eigenvalues ak, $l \geq k \geq 0$, each with multiplicity $\binom{l}{k}(a-1)^k$. The k-th eigenspace can be interpreted as the space of all energy landscapes of interaction order k.

Appendix B.2 Orthogonality of ΔG_{epi} and ΔG_{add}

Before we derive the results shown in Figure 3, we pause to show that with the constraint on the coefficients β defined previously, $\Delta\mathrm{G}_{\mathrm{add}}$ and $\Delta\mathrm{G}_{\mathrm{epi}}$ are contained in orthogonal eigenspaces therefore are mutually orthogonal and also orthogonal to the eigenspaces of higher order interactions.

Appendix B.2.1 $\Delta\mathrm{G}_{\mathrm{add}}$

Recall the definition:

$$\Delta\mathrm{G}_{\mathrm{add}}(x) = \sum_{k=1}^{l} \beta_{\{k\},x_k}. \tag{A15}$$

We first split the vector $\Delta\mathrm{G}_{\mathrm{add}}$ into its constant and linear components:

$$\Delta\mathrm{G}_{\mathrm{lin}} \equiv \Delta\mathrm{G}_{\mathrm{add}} - l\mu_{\mathrm{add}}\mathbf{1}, \tag{A16}$$

where $\mathbf{1}$ denote the column vector with all one's. For any graph Laplacian, $L\mathbf{1} = 0$, therefore the constant part of $\Delta\mathrm{G}_{\mathrm{add}}$ is in the null space of L, which is equivalent to the eigenspace associated with eigenvalue zero. Furthermore, according to equation A14:

$$\begin{aligned}
(L\Delta\mathrm{G}_{\mathrm{lin}})(x) &= l(a-1)\Delta\mathrm{G}_{\mathrm{lin}}(x) - \sum_{x' \sim x} \Delta\mathrm{G}_{\mathrm{lin}}(x') \\
&= l(a-1)\Delta\mathrm{G}_{\mathrm{lin}}(x) + l^2(a-1)\mu_{\mathrm{add}} - \sum_{x' \sim x} \sum_{k=1}^{l} \beta_{\{k\},\{x'_k\}} \\
&= l(a-1)\Delta\mathrm{G}_{\mathrm{lin}}(x) + l^2(a-1)\mu_{\mathrm{add}} - \sum_{k=1}^{l} \sum_{x' \sim x} \beta_{\{k\},\{x'_k\}} \\
&= l(a-1)\Delta\mathrm{G}_{\mathrm{lin}}(x) + l^2(a-1)\mu_{\mathrm{add}} - \sum_{k=1}^{l} \Big((l-1)(a-1)\beta_{\{k\},\{x_k\}} + \sum_{\alpha \in \mathcal{A} \setminus \{x_k\}} \beta_{\{k\},\{\alpha\}} \Big) \\
&= l(a-1)\Delta\mathrm{G}_{\mathrm{lin}}(x) + l^2(a-1)\mu_{\mathrm{add}} - \sum_{k=1}^{l} \Big((l-1)(a-1)\beta_{\{k\},\{x_k\}} + a\,\mu_{\mathrm{add}} - \beta_{\{k\},\{x_k\}} \Big) \\
&= l(a-1)\Delta\mathrm{G}_{\mathrm{lin}}(x) - \sum_{k=1}^{l} \Big(((l-1)(a-1)-1)\beta_{\{k\},\{x_k\}} - (l(a-1)-a)\mu_{\mathrm{add}} \Big) \\
&= l(a-1)\Delta\mathrm{G}_{\mathrm{lin}}(x) - \big(l(a-1)-a\big) \sum_{k=1}^{l} \Big(\beta_{\{k\},\{x_k\}} - \mu_{\mathrm{add}} \Big) \\
&= l(a-1)\Delta\mathrm{G}_{\mathrm{lin}}(x) - \big(l(a-1)-a\big)\Delta\mathrm{G}_{\mathrm{lin}}(x) \\
&= a\Delta\mathrm{G}_{\mathrm{lin}}(x)
\end{aligned}$$

On the fourth line, for each choice of site k, we group the sequences that are adjacent to x into two groups. The first group consist of $(l-1)(a-1)$ sequences that are identical to the focal x on site k, so have coefficient $\beta_{\{k\},\{x_k\}}$. The other group consist of the rest $a-1$ sequences that differ from x at site k.

So we need to sum through $\alpha \in \mathcal{A}\backslash\{x_k\}$. Due to the constraint that $\frac{1}{a}\sum_{\alpha=0}^{a-1}\beta_{\{k\},\{\alpha\}} = \mu_{\text{add}}$, this sum must be equal to $a\,\mu_{\text{add}} - \beta_{\{k\},\{x_k\}}$. Then on the seventh line we also note that $(l-1)(a-1)-1 = l(a-1)-a$. Thus, we conclude that $\Delta\text{G}_{\text{lin}}$ is an eigenvector of L with eigenvalue a.

To summarize, we have shown that the constant and linear part of $\Delta\text{G}_{\text{add}}$ belong to the zeroth and first eigenspace of L with eigenvalues 0 and a, respectively. We also note that since $L\Delta\text{G}_{\text{add}} = a\Delta\text{G}_{\text{lin}} = a\Delta\text{G}_{\text{add}} - a\beta_{\emptyset}$, $\Delta\text{G}_{\text{add}}$ is an "elementary" landscape [46,47].

Appendix B.2.2 $\Delta\text{G}_{\text{epi}}$

Next, we verify that $\Delta\text{G}_{\text{epi}}$ is an eigenvector of the graph Laplacian L with eigenvalue $2a$. The spirit is the same as with $\Delta\text{G}_{\text{lin}}$. First note that $(L\Delta\text{G}_{\text{epi}})(x) = l(a-1)\Delta\text{G}_{\text{epi}}(x) - \sum_{x'\sim x}\Delta\text{G}_{\text{epi}}(x')$. The second term can be expanded as:

$$\sum_{x'\sim x}\Delta\text{G}_{\text{epi}}(x') = \sum_{x'\sim x}\sum_{k_2<k_1}\beta_{\{k_1,k_2\},\{x'_{k_1},x'_{k_2}\}} = \sum_{k_2<k_1}\sum_{x'\sim x}\beta_{\{k_1,k_2\},\{x'_{k_1},x'_{k_2}\}} \tag{A17}$$

$$= \sum_{k_2<k_1}\Big((l-2)(a-1)\beta_{\{k_1,k_2\},\{x_{k_1},x_{k_2}\}} + \sum_{\alpha_1\in\mathcal{A}\backslash\{x_{k_1}\}}\beta_{\{k_1,k_2\},\{\alpha_1,x_{k_2}\}} \tag{A18}$$

$$+ \sum_{\alpha_2\in\mathcal{A}\backslash\{x_{k_2}\}}\beta_{\{k_1,k_2\},\{x_{k_1},\alpha_2\}}\Big) \tag{A19}$$

$$= \sum_{k_2<k_1}\Big((l-2)(a-1)\beta_{\{k_1,k_2\},\{x_{k_1},x_{k_2}\}} - 2\beta_{\{k_1,k_2\},\{x_{k_1},x_{k_2}\}}\Big) \tag{A20}$$

$$= \sum_{k_2<k_1}\big((l-2)(a-1)-2\big)\beta_{\{k_1,k_2\},\{x_{k_1},x_{k_2}\}} \tag{A21}$$

$$= \big((l-2)(a-1)-2\big)\Delta\text{G}_{\text{epi}}(x) \tag{A22}$$

, where on the third line we divide the sequences that are adjacent to x into three groups. The first group consist of $(l-2)(a-1)$ sequences that are identical to the focal x on the two sites that are chosen, so have the same coefficient as x: $\beta_{\{k_1,k_2\},\{x_{k_1},x_{k_2}\}}$. The other two groups each consist of sequences that differ from x at site k_1 or k_2. Due to the constraint that $\sum_{\alpha\in\mathcal{A}}\beta_{\{k_1,k_2\},\{\alpha_1,\alpha_2\}} = 0$ for $\alpha = \alpha_1, \alpha_2$, the sum through the $a-1$ sequences that differ from x on each site must be equal to $-\beta_{\{k_1,k_2\},\{x_{k_1},x_{k_2}\}}$

Therefore,

$$(L\Delta\text{G}_{\text{epi}})(x) = l(a-1)\Delta\text{G}_{\text{epi}}(x) - \sum_{x'\sim x}\Delta\text{G}_{\text{epi}}(x') \tag{A23}$$

$$= \big(l(a-1) - (l-2)(a-1) + 2\big)\Delta\text{G}_{\text{epi}}(x) \tag{A24}$$

$$= 2a\Delta\text{G}_{\text{epi}}(x). \tag{A25}$$

We have shown that $\Delta\text{G}_{\text{lin}}$ and $\Delta\text{G}_{\text{epi}}$ are eigenvectors of the graph Laplacian L and have eigenvalues a and $2a$, respectively. Therefore they are mutually orthogonal, and furthermore $\Delta\text{G}_{\text{epi}}$ is orthogonal to $\Delta\text{G}_{\text{add}}$, since $\Delta\text{G}_{\text{add}}$ is contained in the union of the eigenspaces corresponding to 0 and a, whereas $\Delta\text{G}_{\text{epi}}$ is in the eigenspace corresponding to eigenvalue $2a$. Furthermore, all of $\Delta\text{G}_{\text{add}}$, $\Delta\text{G}_{\text{lin}}$ and $\Delta\text{G}_{\text{epi}}$ are orthogonal to eigenspaces spanned by interactions of order greater than 2.

Appendix B.3 Expected variance in energy of distance classes under the random field model

We now derive the results shown in Figure 3. For a sequence $x \in \mathcal{S}$, its energy under a general random field model is [20,21]

$$f(x) = \sum_{k=0}^{l} \sum_{i=1}^{\binom{l}{k}(a-1)^k} b_{k_i}\phi_{k_i}(x), \tag{A26}$$

where $\{\phi_{k_i}\}_{l\geq k\geq 0}$ is the set of orthonormal basis functions that spans $\mathbb{R}^{\mathcal{S}}$ and ϕ_{k_i} is the i-th basis function of interaction order k. $\{b_{k_i}\}$ are random variables representing the interaction coefficients. Here we choose $\{\phi_{k_i}\}$ to be eigenvectors of the the graph Laplacian L associated with $\mathcal{G}$.

For simplicity, here we only consider models with interactions of a certain order $k \geq 1$, so

$$f(x) = \sum_i b_{k_i}\phi_{k_i}(x). \tag{A27}$$

Since the $\{b_{k_i}\}$ of different orders are statistically independent, to simplify the notation, we derive the following results for energy landscapes with only k-th order interactions and only consider landscapes with multiple orders of interaction at the end. In our random field model, the coefficients b_{k_i}'s for a given k are drawn i.i.d from some distribution with mean 0 and variance σ_k^2. Without loss of generality, we set $\sigma_k^2 = 1$. So we have

$$f \sim \mathcal{D}(0, W), \tag{A28}$$

where W is the covariance matrix. The distribution $\mathcal{D}$ is not specified here because we are only concerned with the first and second moment. The covariance matrix W only depends on $\mathbf{d}(x, x')$ and its entries are given by:

$$\begin{aligned}
\sigma_{f(x)f(x')} &= E[\sum_i b_{k_i}\phi_{k_i}(x) \sum_j b_{k_j}\phi_{k_j}(x')] && \text{(A29)}\\
&= \sum_{i,j} E[b_{k_i}b_{k_j}]\phi_{k_i}(x)\phi_{k_j}(x') && \text{(A30)}\\
&= \sum_i E[b_{k_i}^2]\phi_{k_i}(x)\phi_{k_i}(x') && \text{(A31)}\\
&= \sum_i \phi_{k_i}(x)\phi_{k_i}(x') && \text{(A32)}\\
&= \sum_{q=0}^{\min\{k,\mathbf{d}(x,x')\}} a^{-l}(-1)^q(a-1)^{k-q}\binom{\mathbf{d}(x,x')}{q}\binom{l-\mathbf{d}(x,x')}{k-q} && \text{(A33)}\\
&\equiv w_k(\mathbf{d}(x,x')) && \text{(A34)}
\end{aligned}$$

The second to last step is not obvious but is well known in coding theory and some theoretical studies of fitness landscape and is commonly referred to as the Krawtchouk polynomial [20,48].

For an energy landscape f drawn from the above distribution, the sample variance of energies of all sequences at distance $l \geq d > 0$ to wt is:

$$V(\{f(x)|x \in S(\text{wt}, d)\}) \equiv V(d) = \frac{1}{n} \sum_{x\in S(\text{wt},d)} (f(x) - \langle f(x')\rangle_{S(\text{wt},d)})^2 \tag{A35}$$

Here, we use $\langle\cdot\rangle_T$ to denote the mean taken over the set T. $S(\text{wt}, d) = \{x \in \mathcal{S}|\mathbf{d}(x, \text{wt}) = d\}$ is the set of all sequences at distance d to wt and $|S(\text{wt}, d)| = \binom{l}{d}(a-1)^d = n$.

Using a well-known expression for the expected sample variance, we can write [49]:

$$E[V(d)] = \frac{n-1}{n}(\overline{\sigma^2}_d + \sigma_{d,\mu}^2 - \overline{\sigma}_d). \tag{A36}$$

The three quantities are:

$$\overline{\sigma^2}_d = \frac{1}{n} \sum_{x \in S(\mathrm{wt},d)} \sigma^2_{f(x)} \tag{A37}$$

$$\sigma^2_{d,\mu} = \frac{1}{n-1} \sum_{x \in S(\mathrm{wt},d)} (E[f(x)] - \frac{1}{n} \sum_{x' \in S(\mathrm{wt},d)} E[f(x')])^2 \tag{A38}$$

$$\overline{\sigma}_d = \langle \sigma_{f(x)f(x')} \rangle_{\{(x,x') \in S^2(\mathrm{wt},d) | x \neq x'\}}. \tag{A39}$$

We now turn to deriving each of these three quantities individually.

First, we have the mean of variances $\overline{\sigma^2}_d$ for sequences at distance d to wt. By setting $d = 0$ in the Krawchouk polynomial:

$$\sigma^2_{f(x)} = w_k(0) = a^{-l} \binom{l}{k} (a-1)^k \sigma^2_k = a^{-l} \binom{l}{k} (a-1)^k, \tag{A40}$$

for all $x \in S(\mathrm{wt}, d)$. $\binom{l}{k}(a-1)^k$ is the number of k-th order interactions. And the last step was simplified by setting $\sigma^2_k = 1$.

Next, we have $\sigma^2_{d,\mu}$, which is the variance of the mean energy, $E[f(x)]$, of sequences in $S(\mathrm{wt}, d)$. Since $E[f(x)]$ is constant across all $x \in S(\mathrm{wt}, d)$, we have

$$\sigma^2_{d,\mu} = 0. \tag{A41}$$

Last is the mean covariance between energies of sequences $x, x' \in S(\mathrm{wt}, d)$, $x \neq x'$:

$$\begin{aligned}
\overline{\sigma}_d &= \langle \sigma_{f(x)f(x')} \rangle_{\{(x,x') \in S^2(\mathrm{wt},d) | x \neq x'\}} && \text{(A42)}\\
&= \frac{1}{\binom{l}{d}(a-1)^d} \sum_{x \in S(\mathrm{wt},d)} \langle \sigma_{f(x)f(x')} \rangle_{\{x' | \mathbf{d}(x',\mathrm{wt})=d, x' \neq x\}} && \text{(A43)}\\
&= \langle \sigma_{f(x)f(x')} \rangle_{\{x' | \mathbf{d}(x',\mathrm{wt})=d, x' \neq x\}} && \text{(A44)}\\
&= \frac{1}{\binom{l}{d}(a-1)^d - 1} \sum_{d'=1}^{\min\{l,2d\}} N(d,d') w_k(d') && \text{(A45)}
\end{aligned}$$

Due to the assumption that the covariance structure only depends on d, the summand on the second line is the same for all $x \in S(\mathrm{wt}, d)$. Therefore we can arbitrarily pick a sequence x and calculate a weighted sum with weights given by

$$N(d,d') = |\{x' | \mathbf{d}(\mathrm{wt}, x') = d, \mathbf{d}(x, x') = d'\}| = |S(\mathrm{wt}, d) \cap S(x, d')|, \tag{A46}$$

which is the number of sequences at distance d to wt and d' to x. Note that $N(d, d')$ is the same for all $x \in S(\mathrm{wt}, d)$ so only depends d and d'. The normalizing factor

$$\sum_{d'=1}^{\min\{l,2d\}} N(d,d') = \binom{l}{d}(a-1)^d - 1 \tag{A47}$$

is the total number of sequences in $S(\mathrm{wt}, d)$ minus the focal sequence x.

Our final task is to count $N(d, d')$. First we pick $d \geq s \geq 0$ sites out of d sites on which x and wt differ and set the states of x' on these sites to be the same as wt. The number of choices: $\binom{d}{s}$. Second, since $\mathbf{d}(x', \mathrm{wt}) = d$, we must choose s sites out of the $l - d$ sites where x and wt are identical and set them to be one of the $a - 1$ states for x'. The number of choices is $\binom{l-d}{s}(a-1)^s$. Third, now we have x and x' differ on $2s$ sites and since $\mathbf{d}(x, x') = d'$, we need to choose $d' - 2s$ sites for x' out of the $d - s$

Table A1. A simple example for counting $N(d, d')$, with $\mathbf{d}(\text{wt}, x) = \mathbf{d}(\text{wt}, x') = 6$, and $\mathbf{d}(x, x') = 4$.

wt	0	0	0	0	0	0	0	0	0	0	0	0	0	0	0
x	0	0	0	0	0	0	0	0	0	1	1	1	1	1	1
x'	0	0	0	0	0	0	0	1	1	1	1	2	2	0	0

sites whose states we have not decided yet and set the states of x' to be one of the $a-2$ states that is different from both x and wt. The number of choices is $\binom{d-s}{d'-2s}(a-2)^{d'-2s}$

Putting these together we have

$$N(d, d') = \sum_{s=0}^{\min\{d, \lfloor \frac{d'}{2} \rfloor\}} \binom{d}{s}\binom{l-d}{s}(a-1)^s \binom{d-s}{d'-2s}(a-2)^{d'-2s}, \tag{A48}$$

and so finally we have:

$$\frac{n}{n-1}E[V(d)] = \overline{\sigma^2}_d + \sigma^2_{d,\mu} - \overline{\sigma}_d \tag{A49}$$

$$= a^{-l}\binom{l}{k}(a-1)^k - \frac{1}{\binom{l}{d}(a-1)^d - 1}\sum_{d'=1}^{\min\{l,2d\}} N(d, d')w_k(d') \tag{A50}$$

$$= w_k(0) - \frac{1}{\binom{l}{d}(a-1)^d - 1}\sum_{d'=1}^{\min\{l,2d\}} N(d, d')w_k(d'). \tag{A51}$$

It may be possible to further simplify this expression by plugging in $N(d, d')$ and $w_k(d')$ so that it is more intelligible. But calculation of $E[V(d)]$ based on this expression is computationally feasible since both $N(d, d')$ and $w_k(d)$ are easy to calculate.

We have derived the results above for energy landscapes with only k-th order interactions and by setting $\sigma_k^2 = 1$. For an energy landscape with all orders of interactions with Walsh coefficients b_{k_i}'s drawn i.i.d with mean 0 and variance σ_k^2 for each order k,

$$E[V(d)] = \frac{1}{1 - \binom{l}{d}^{-1}(a-1)^{-d}}\sum_{k=0}^{l}\sigma_k^2\Big(w_k(0) - \frac{1}{\binom{l}{d}(a-1)^d - 1}\sum_{d'=1}^{\min\{l,2d\}} N(d, d')w_k(d')\Big). \tag{A52}$$

Appendix C

Appendix C.1 Bivariate normal approximation

We approximate $(\Delta G_{\text{add}}, \Delta G_{\text{epi}})$ with a bivariate normal distribution with mean vector

$$(\mu_1, 0) := (l\mu_{\text{add}}, 0) \tag{A53}$$

and covariance matrix

$$\begin{pmatrix} \sigma_1^2 & 0 \\ 0 & \sigma_2^2 \end{pmatrix} := \begin{pmatrix} l\frac{\alpha-1}{\alpha}\sigma^2_{\text{add}} & 0 \\ 0 & \binom{l}{2}\frac{(\alpha-1)^2}{\alpha^2}\sigma^2_{\text{epi}} \end{pmatrix}, \tag{A54}$$

where the parameters were chosen according to the procedure described in Appendix A. Therefore, in this approximation, the total folding energy $\Delta G = \Delta G_{\text{add}} + \Delta G_{\text{epi}}$ is also normally distributed, with mean $\mu := \mu_1$ and variance $\sigma^2 := \sigma_1^2 + \sigma_2^2$. Using this normal approximation, we give an analytical justification for the phenomenon observed in Figure 2, that although the effect of epistasis is small, it is nonetheless crucial for folding. The analytical formulas we obtain for describing this phenomenon will also specify the regime of model parameters for which we can expect to see the phenomenon. We

shall use two quantities to measure the strength of this phenomenon. For the smallness of the epistatic effect, we use the measure σ_2^2/σ^2, the fraction of the variance across all sequences accounted for by the variance of the epistatic energy. For the importance of the epistatic effect, we use the measure $E(\Delta G_{\text{add}}|\Delta G < 0)$, the mean of additive energies of viable sequences. If this mean is far above the viability threshold 0 it indicates that on average epistasis makes a substantial contribution to the ability of viable sequences to fold.

Now, we analytically approximate the conditional expectation $E(\Delta G_{\text{add}}|\Delta G < 0)$. We use a classical result that is refered to as the regression towards the mean formula for a pair of normally distributed random variables. If (X, Y) has normal distribution with mean (μ_X, μ_Y) and covariance matrix

$$\begin{pmatrix} \sigma_X^2 & \rho_{XY}\sigma_X\sigma_Y \\ \rho_{XY}\sigma_X\sigma_Y & \sigma_Y^2 \end{pmatrix},$$

then the regression towards the mean formula describes how the means change if we condition on one of the variables being below some cutoff value c:

$$E(X|Y < c) - E(X) = \rho_{XY}\frac{\sigma_X}{\sigma_Y}\Big(E(Y|Y < c) - E(Y)\Big). \tag{A55}$$

Applying this formula to ΔG and ΔG_{add} and the condition that a sequence is viable, i.e. $\Delta G < 0$, we obtain

$$E(\Delta G_{\text{add}}|\Delta G < 0) - \mu_1 = R^2\Big(E(\Delta G|\Delta G < 0) - \mu\Big), \tag{A56}$$

where

$$R^2 := \frac{\text{Cov}(\Delta G_{\text{add}}, \Delta G)}{\sigma_1\sigma}\frac{\sigma_1}{\sigma} = \frac{\sigma_1^2}{\sigma^2}$$

is calculated using the fact that $\Delta G = \Delta G_{\text{add}} + \Delta G_{\text{epi}}$ and that the additive and epistatic energies are uncorrelated by (A54). Also by (A54), $\mu = \mu_1$, hence we can express the mean additive folding energy of viable sequences from (A56) as

$$E(\Delta G_{\text{add}}|\Delta G < 0) = \left(1 - R^2\right)\mu_1 + R^2 E(\Delta G|\Delta G < 0). \tag{A57}$$

The conditional mean on the right hand side of the equation above can be calculated as

$$E(\Delta G|\Delta G < 0) = \mu - \sigma\frac{\psi\left(-\frac{\mu}{\sigma}\right)}{\Psi\left(-\frac{\mu}{\sigma}\right)}, \tag{A58}$$

where ψ and Ψ are the PDF and CDF, respectively, of the standard normal distribution, and as μ becomes large compared to σ, $E(\Delta G|\Delta G < 0)$ approaches 0.

Returning to (A57), we obtain the estimate

$$E(\Delta G_{\text{add}}|\Delta G < 0) \approx \left(1 - R^2\right)\mu_1 = \frac{\sigma_2^2}{\sigma_1^2 + \sigma_2^2}\mu_1. \tag{A59}$$

This means that no matter how small the epistatic effect is, measured by $\sigma_2^2/(\sigma_1^2 + \sigma_2^2)$, if the mean of the additive energy μ_1 is large enough in comparison, the role of the epistatic energy is crucial for protein folding.

Plugging in our model parameters as given in (A53) and (A54), and using the approximations $\alpha - 1 \approx \alpha$ and $l - 1 \approx l$, the estimate in (A59) becomes

$$\frac{l^2\mu_{\text{add}}\sigma_{\text{epi}}^2}{l\sigma_{\text{epi}}^2 + 2\sigma_{\text{add}}^2}.$$

The choice of parameters $\mu_{\text{add}} = 1$, $\sigma_{\text{add}} = 1$, and $\sigma_{\text{epi}} = 0.0003$ then yield 22.59, which is very close to 22.45, the mean additive energy of sequences observed in the simulation.

1. Sikosek, T.; Chan, H.S. Biophysics of protein evolution and evolutionary protein biophysics. *Journal of The Royal Society Interface* **2014**, *11*, 20140419.
2. Bastolla, U.; Dehouck, Y.; Echave, J. What evolution tells us about protein physics, and protein physics tells us about evolution. *Current opinion in structural biology* **2017**, *42*, 59–66.
3. Starr, T.N.; Thornton, J.W. Epistasis in protein evolution. *Protein Science* **2016**, *25*, 1204–1218.
4. Echave, J.; Wilke, C.O. Biophysical models of protein evolution: understanding the patterns of evolutionary sequence divergence. *Annual review of biophysics* **2017**, *46*, 85–103.
5. Storz, J.F. Compensatory mutations and epistasis for protein function. *Current opinion in structural biology* **2018**, *50*, 18–25.
6. Li, H.; Tang, C.; Wingreen, N.S. Are protein folds atypical? *Proceedings of the National Academy of Sciences* **1998**, *95*, 4987–4990.
7. Tokuriki, N.; Tawfik, D.S. Stability effects of mutations and protein evolvability. *Current opinion in structural biology* **2009**, *19*, 596–604.
8. Taverna, D.M.; Goldstein, R.A. Why are proteins marginally stable? *Proteins: Structure, Function, and Bioinformatics* **2002**, *46*, 105–109.
9. Shakhnovich, E.I. Protein design: a perspective from simple tractable models. *Folding and Design* **1998**, *3*, R45–R58.
10. Govindarajan, S.; Goldstein, R.A. On the thermodynamic hypothesis of protein folding. *Proceedings of the National Academy of Sciences* **1998**, *95*, 5545–5549.
11. Goldstein, R.A. The evolution and evolutionary consequences of marginal thermostability in proteins. *Proteins: Structure, Function, and Bioinformatics* **2011**, *79*, 1396–1407.
12. Serohijos, A.W.; Shakhnovich, E.I. Merging molecular mechanism and evolution: theory and computation at the interface of biophysics and evolutionary population genetics. *Current opinion in structural biology* **2014**, *26*, 84–91.
13. Goldstein, R.A.; Pollock, D.D. Sequence entropy of folding and the absolute rate of amino acid substitutions. *Nature ecology & evolution* **2017**, *1*, 1923.
14. Ashenberg, O.; Gong, L.I.; Bloom, J.D. Mutational effects on stability are largely conserved during protein evolution. *Proc. Natl. Acad. Sci. U. S. A.* **2013**, *110*, 21071–21076.
15. Pollock, D.D.; Thiltgen, G.; Goldstein, R.A. Amino acid coevolution induces an evolutionary Stokes shift. *Proc. Natl. Acad. Sci. U. S. A.* **2012**, *109*, E1352–9.
16. Shah, P.; McCandlish, D.M.; Plotkin, J.B. Contingency and entrenchment in protein evolution under purifying selection. *Proc. Natl. Acad. Sci. U. S. A.* **2015**, *112*, E3226–E3235, [http://www.pnas.org/content/112/25/E3226.full.pdf]. doi:10.1073/pnas.1412933112.
17. Breen, M.S.; Kemena, C.; Vlasov, P.K.; Notredame, C.; Kondrashov, F.A. Epistasis as the primary factor in molecular evolution. *Nature* **2012**, *490*, 535–538.
18. Wells, J.A. Additivity of mutational effects in proteins. *Biochemistry* **1990**, *29*, 8509–8517.
19. Risso, V.A.; Manssour-Triedo, F.; Delgado-Delgado, A.; Arco, R.; Barroso-delJesus, A.; Ingles-Prieto, A.; Godoy-Ruiz, R.; Gavira, J.A.; Gaucher, E.A.; Ibarra-Molero, B.; Sanchez-Ruiz, J.M. Mutational Studies on Resurrected Ancestral Proteins Reveal Conservation of Site-Specific Amino Acid Preferences throughout Evolutionary History. *Mol. Biol. Evol.* **2015**, *32*, 440–455, [http://mbe.oxfordjournals.org/content/32/2/440.full.pdf+html]. doi:10.1093/molbev/msu312.
20. Stadler, P.F.; Happel, R. Random field models for fitness landscapes. *Journal of Mathematical Biology* **1999**, *38*, 435–478. doi:10.1007/s002850050156.
21. Neidhart, J.; Szendro, I.G.; Krug, J. Exact results for amplitude spectra of fitness landscapes. *Journal of Theoretical Biology* **2013**, *332*, 218–227.
22. Aita, T.; Uchiyama, H.; Inaoka, T.; Nakajima, M.; Kokubo, T.; Husimi, Y. Analysis of a local fitness landscape with a model of the rough Mt. Fuji-type landscape: Application to prolyl endopeptidase and thermolysin. *Biopolymers* **2000**, *54*, 64–79.

23. Neidhart, J.; Szendro, I.G.; Krug, J. Adaptation in tunably rugged fitness landscapes: the rough Mount Fuji model. *Genetics* **2014**, *198*, 699–721.
24. Kingman, J. A simple model for the balance between selection and mutation. *Journal of Applied Probability* **1978**, *15*, 1–12.
25. Guerois, R.; Nielsen, J.E.; Serrano, L. Predicting changes in the stability of proteins and protein complexes: a study of more than 1000 mutations. *Journal of molecular biology* **2002**, *320*, 369–387.
26. Miyazawa, S.; Jernigan, R.L. Residue–residue potentials with a favorable contact pair term and an unfavorable high packing density term, for simulation and threading. *Journal of molecular biology* **1996**, *256*, 623–644.
27. Chan, H.; Bornberg-Bauer, E. Perspectives on protein evolution from simple exact models. *Applied bioinformatics* **2002**, *1*, 121–144.
28. Tokuriki, N.; Stricher, F.; Schymkowitz, J.; Serrano, L.; Tawfik, D.S. The stability effects of protein mutations appear to be universally distributed. *Journal of molecular biology* **2007**, *369*, 1318–1332.
29. Zeldovich, K.B.; Chen, P.; Shakhnovich, E.I. Protein stability imposes limits on organism complexity and speed of molecular evolution. *Proceedings of the National Academy of Sciences* **2007**, *104*, 16152–16157.
30. Wylie, C.S.; Shakhnovich, E.I. A biophysical protein folding model accounts for most mutational fitness effects in viruses. *Proceedings of the National Academy of Sciences* **2011**, *108*, 9916–9921.
31. Miyazawa, S. Selection maintaining protein stability at equilibrium. *Journal of theoretical biology* **2016**, *391*, 21–34.
32. Bloom, J.D.; Raval, A.; Wilke, C.O. Thermodynamics of Neutral Protein Evolution. *Genetics* **2007**, *175*, 255 – 266, [http://www.genetics.org/content/175/1/255.full.pdf+html]. doi:10.1534/genetics.106.061754.
33. Serrano, L.; Day, A.G.; Fersht, A.R. Step-wise mutation of barnase to binase: a procedure for engineering increased stability of proteins and an experimental analysis of the evolution of protein stability. *Journal of molecular biology* **1993**, *233*, 305–312.
34. Serohijos, A.W.; Shakhnovich, E.I. Contribution of selection for protein folding stability in shaping the patterns of polymorphisms in coding regions. *Molecular biology and evolution* **2013**, *31*, 165–176.
35. van Nimwegen, E.; Crutchfield, J.P.; Huynen, M. Neutral evolution of mutational robustness. *Proc. Natl. Acad. Sci. U. S. A.* **1999**, *96*, 9716 – 9720.
36. Galton, F. Regression towards mediocrity in hereditary stature. *The Journal of the Anthropological Institute of Great Britain and Ireland* **1886**, *15*, 246–263.
37. Lynch, M.; Walsh, B.; others. *Genetics and analysis of quantitative traits*; Vol. 1, Sinauer Sunderland, MA, 1998.
38. Kimura, M.; Crow, J.F. Effect of overall phenotypic selection on genetic change at individual loci. *Proceedings of the National Academy of Sciences* **1978**, *75*, 6168–6171.
39. Draghi, J.A.; Plotkin, J.B. Selection biases the prevalence and type of epistasis along adaptive trajectories. *Evolution* **2013**, *67*, 3120–3131.
40. Greene, D.; Crona, K. The changing geometry of a fitness landscape along an adaptive walk. *PLoS computational biology* **2014**, *10*, e1003520.
41. Blanquart, F.; Achaz, G.; Bataillon, T.; Tenaillon, O. Properties of selected mutations and genotypic landscapes under Fisher's geometric model. *Evolution* **2014**, *68*, 3537–3554.
42. Drummond, D.A.; Wilke, C.O. Mistranslation-induced protein misfolding as a dominant constraint on coding-sequence evolution. *Cell* **2008**, *134*, 341–352.
43. Gavrilets, S.; Gravner, J. Percolation on the fitness hypercube and the evolution of reproductive isolation. *J. Theor. Biol.* **1997**, *184*, 51 – 64.
44. Wunderlich, Z.; Mirny, L.A. Different gene regulation strategies revealed by analysis of binding motifs. *Trends in genetics* **2009**, *25*, 434–440.
45. Socolich, M.; Lockless, S.W.; Russ, W.P.; Lee, H.; Gardner, K.H.; Ranganathan, R. Evolutionary information for specifying a protein fold. *Nature* **2005**, *437*, 512.
46. Vassilev, V.K.; Fogarty, T.C.; Miller, J.F. Smoothness, ruggedness and neutrality of fitness landscapes: from theory to application. In *Advances in evolutionary computing*; Springer, 2003; pp. 3–44.
47. Stadler, P.F. Landscapes and their correlation functions. *Journal of Mathematical Chemistry* **1996**, *20*, 1–45.
48. Van Lint, J.H. *Introduction to coding theory*; Vol. 86, Springer Science & Business Media, 2012.

49. Bradley, R.S. Estimation of bias and variance of measurements made from tomography scans. *Measurement Science and Technology* **2016**, 27. doi:10.1088/0957-0233/27/9/095402.

© 2018 by the authors. Submitted to *Genes* for possible open access publication under the terms and conditions of the Creative Commons Attribution (CC BY) license (http://creativecommons.org/licenses/by/4.0/).